ARTICLE NO. 79-0013R

J80-144

Time-Dependent Method to Solve the Inverse Problem for Internal Flows

L. Zannetti*
Politecnico di Torino, Turin, Italy

The objective of this paper is a numerical method for designing ducts with arbitrary prescribed pressure distribution at the walls. The method applies to inviscid compressible subsonic or transonic, two-dimensional or axisymmetric flows, and it is based on the time-dependent technique. The walls where the pressure distribution is prescribed are considered as flexible and impermeable. Starting from some initial guessed configuration, the computation follows the transient which occurs while the flexible walls move and finally reach a steady shape. Several numerical examples are described and compared with the solution of the direct problem in the case of two-dimensional and axisymmetric subsonic diffusers, transonic nozzles and elbows.

Nomenclature

a	= speed of sound
b,c	= see Fig. 1
c_v	= constant volume specific heat
l	= length
p	= pressure
q	= velocity
$u,w,\tilde{u},\tilde{w}$	= velocity components (see Fig. 2)
t	= time
x,z	= rectangular coordinates
P	= logarithm of pressure
R	= gas constant
S	= entropy
T	= temperature
X,Z,τ	= transformed coordinates
γ	= specific heats ratio
θ	= angle in the polar frame of reference
ϕ	= see Fig. 2
ψ	= stream function

All quantities are normalized with respect to reference values: $l_{ref}, p_{ref}, T_{ref}, q_{ref}=\sqrt{RT_{ref}}, t_{ref}=(l_{ref}/q_{ref}), S_{ref}=c_v$.

I. Introduction

THE inverse problem for internal flow consists in the determination of the shape that the walls of a duct have to assume once the pressure acting on them is given.

The classic solution of the inverse problem is due to Stanitz[1] for the case of the two-dimensional potential flow. The Stanitz solution has been extended to the axisymmetric potential flow by Nelson et al.[2] Such solutions are based on the treatment of the potential and stream functions, therefore they are confined to the two-dimensional or axisymmetric potential flows.

The present method is based on the numerical solution of the full Euler equations for the unsteady motion. It applies to all the inviscid compressible flows and even if the results presented here refer to two-dimensional or axisymmetric flows, it does not present any conceptual or practical limitation to the extension to three-dimensional flows.

II. General Description of the Method

The method here proposed is the general extension of the procedure shown in Ref. 3. It is based on the idea of the time-dependent technique and is very similar to the algorithm used in the solution of the direct problem.

In the direct problem the geometry of the duct is prescribed, then some initial flow configuration is guessed and the steady flowfield configuration is obtained asymptotically in time, at the end of a transient. In particular, the pressure distribution along the rigid walls will vary during the transient, until the final steady distribution of pressure is achieved.

In the inverse problem a duct with flexible and impermeable walls is considered, their shape can vary in time, but the pressure acting on these is prescribed as boundary condition. During the transient the flexible walls move in a wavy fashion and at the end they will assume the steady shape required by the prescribed pressure and in agreement with the steady internal flow.

Whereas in the Stanitz solution the pressure is prescribed as function of the arc length, here the pressure is given as function of one spatial variable, for instance in an axisymmetric nozzle the pressure at the wall is given as function of the axis length or in an elbow as function of the angle in a polar frame of reference.

A coordinate transformation is used in order to map the physical region, whose shape depends on time, into a computational domain, whose shape is independent of time, as is usual in this kind of problems (see for example, Ref. 4).

The full Euler equations of the unsteady flow are hyperbolic partial differential equations, they are integrated in time by means of a finite-difference procedure, according to the second-order-accuracy predictor-corrector scheme suggested by McCormack.[5]

Figure 1 shows one of the possible patterns that can be studied. The domain is bounded by the solid wall AB, the flexible wall CD, the entry permeable surface AC, and the exit permeable surface BD. The flexible wall is constrained at the point C, while the point D can move along the exit surface BD.

The details of the way the entry and exit surfaces act on the flow and the algorithm used on these boundaries are described in Ref. 6. Briefly, they act as discontinuity surfaces and quasisteady relationships hold through them. In front of the AC boundary, the total pressure and temperature are prescribed, while behind it the flow angles are given. These

Presented as Paper 79-0013 at the AIAA 17th Aerospace Sciences Meeting, New Orleans, La., Jan. 15-17, 1979; submitted Feb. 21, 1979; revision received Dec. 4, 1979.

Index categories: Computational Methods; Nozzle and Channel Flow; Transonic Flow.

*Associate Professor, Aeronautical Engineering.

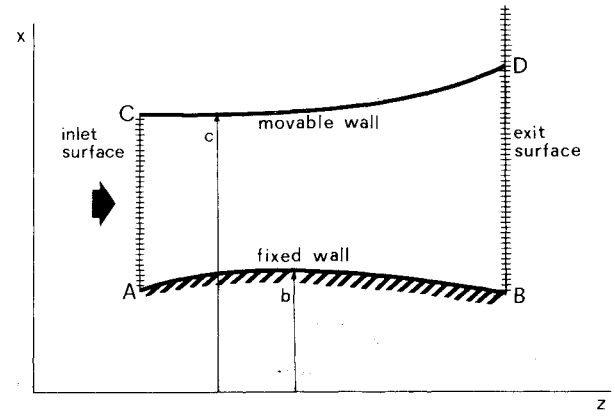

Fig. 1 The physical model.

conditions are matched with a compatibility equation in order to compute the evolution in time of the static pressure and velocity. In a similar way, in the case the flow is subsonic, the flow variables are computed at the exit surface BD, once the discharging static pressure and the flow angles are prescribed behind it. In the case where the flow is supersonic at the exit, it does not depend on the downstream conditions and the computation here depends only on the upstream flow.

Such surfaces are not essential to the inverse problem solution; a proper stretching may extend the physical domain to infinity. In any event, they are very useful in limiting the mesh points, i.e., the computational time, and they easily allow the simulation of a large number of different inlet or exit conditions, as pointed out in Ref. 6.

Figure 1 does not represent the only possible pattern, but as will be shown later both impermeable walls may be movable or be partly movable and partly solid, in order to solve the intermediate problem (the pressure is prescribed on one part of the wall whereas the wall geometry is given on the other).

III. The Equations

With reference to Fig. 1, let c be the ordinate of the upper wall and b the ordinate of the lower wall. In the more general case, c and b depend on the time t and on the abscissa z.

$$b=b(t,z)$$

$$c=c(t,z)$$

Through the transformation:

$$X=\frac{x-b}{c-b};\quad Z=z;\quad \tau=t$$

the impermeable walls b,c of the physical planes x,z are mapped on the straight lines $X=0$, $X=1$ of the computational plane X,Z; hence the physical domain, whose shape may vary during the transient, is mapped into a rectangular region whose shape is independent of time.

The equations of the motion (two-dimensional or axisymmetric), written on the computational frame, are:

$$P_\tau+AP_X+wP_Z+\gamma\left(u_X X_x+w_X X_z+w_Z+j\frac{u}{x}\right)=0$$

continuity $\begin{cases} j=0 & \text{two-dimensional case} \\ j=1 & \text{axisymmetric} \end{cases}$

$$\left.\begin{aligned} &u_\tau+Au_X+wu_Z+TP_X X_x=0 \\ &w_\tau+Aw_X+ww_Z+T(P_X X_z+P_Z)=0 \end{aligned}\right\}\ \text{momentum} \qquad (1)$$

$$S_\tau+AS_X+wS_Z=0 \qquad \text{energy}$$

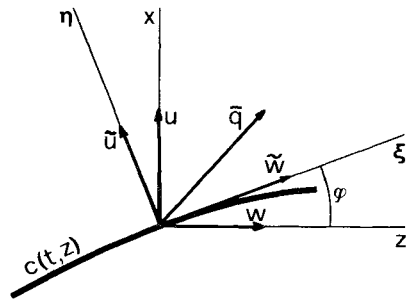

Fig. 2 The movable wall.

where:

$$A=X_t+uX_x+wX_z$$

and

$$X_x=1/(c-b);\quad X_z=X_x[-b_z-X(c_z-b_z)];$$

$$X_t=X_x[-b_t-X(c_t-b_t)]$$

The velocity components u,w; the logarithm of pressure P, and the entropy S are computed on the mesh points of the computational plane by integrating Eqs. (1) in time. At each time step the computed values are ascribed back to the corresponding physical points, once the movable wall locations b,c are computed.

IV. Computation at the Movable Boundary

For the sake of simplicity, let us suppose only the upper wall is movable. Besides the flow variables (u,w,P,S), the location of the wall c and its slope c_z have to be computed at each time step. Figure 2 shows a sketch of the movable wall. A local frame of reference (ξ,η), normal and tangential to the boundary and movable with it, is adopted. The components of the velocity $\bar{q}$ in the new frame are:

$$\tilde{u}=-wN_2+uN_1$$

$$\tilde{w}=wN_1+uN_2$$

where:

$$N_1=\cos\phi;\quad N_2=\sin\phi$$

By combining the continuity and momentum equations, a compatibility equation is gotten along a characteristic line of the reference plane (X,τ), which impinges on the boundary from the inner points:

$$P_\tau+\lambda P_X+\frac{\gamma}{a}(\tilde{u}_\tau+\lambda\tilde{u}_X)=B \qquad (2)$$

where:

$$\lambda=a(X_x/N_1)$$

$$B=-wP_Z-\gamma\left(w_Z+j\frac{u}{x}\right)-\frac{\gamma}{a}[TP_Z N_2$$

$$-\tilde{w}N_1^2 c_{\tau Z}-w(u_Z N_1-w_Z N_2)]$$

The movable wall has to satisfy the condition of impermeability, therefore it has to move with the velocity:

$$c_\tau=(\tilde{u}/N_1) \qquad (3)$$

By substituting the time derivative of Eq. (3) in Eq. (2), one has:

$$c_{\tau\tau}=\frac{\gamma/a(\tilde{u}N_1N_2c_{\tau Z}-\lambda\tilde{u}_X)-(P_\tau+\lambda P_X)+B}{N_1\gamma/a} \tag{4}$$

where the time derivative of the pressure P_τ is given as boundary condition. (In many aspects this procedure follows the ideas presented in Ref. 7 for the explicit treatment of shocks.) The momentum equation along this boundary is:

$$\tilde{w}_\tau=\tilde{u}N_1^2c_{\tau Z}-w(u_ZN_2+w_ZN_1)-TN_1P_Z \tag{5}$$

The new value of the velocity of the wall c_τ is achieved by integrating Eq. (4) and the new value of the wall location c is obtained by the further integration of c_τ. The new value of the velocity component $\tilde{w}$ is gotten by integrating Eq. (5). The new value of the slope $c_Z=\tan\phi$ of the wall is evaluated by the finite-difference approximation on the new values of the wall location c. It is then possible to decode the new values of the velocity components u,w from c_z, c_τ, and $\tilde{w}$:

$$u=c_\tau\cos^2\phi+\tilde{w}\sin\phi$$

$$w=-c_\tau\cos\phi\sin\phi+\tilde{w}\cos\phi$$

The integration of the energy equation provides the new value of the entropy.

The numerical algorithm follows the two-step predictor corrector scheme, as well as at the interior points. Dumping or artificial smoothing devices are not used, and the computation gets strong stability by evaluating the Z derivatives c_Z and $c_{\tau Z}$ in terms of upwind differences. Therefore, when the McCormack algorithm would ask for a downstream difference, the c_Z derivative, for instance, is computed at the point N according to the formula:

$$c_Z=\frac{2c_N-3c_{N-1}+c_{N-2}}{\Delta Z}$$

which preserves the second-order-accuracy of the computation.

A special algorithm is required for the computation of point D (see Fig. 1) in the case where the flow is subsonic. As mentioned above, a discontinuity surface is located at the exit. The static pressure and the slope of the particle path are prescribed downstream of it and the quasisteady relationships of conservation of the mass flow, total temperature and total pressure hold through it. At point D the pressure is prescribed on both the sides of the discontinuity, D being a point of the movable wall, as well as a point of the exit surface. By assuming the same pressure value on the two sides, the slope of the particle path in front of the discontinuity has to be equal to the downstream prescribed slope. For the sake of simplicity, let the slope be zero. It follows that the velocity component u has to be zero and that

$$c_\tau=-wc_Z$$

By taking the time derivative, one has:

$$c_{\tau\tau}=-w_\tau c_Z-wc_{\tau Z}$$

where w_τ is computed, as are the other points of the exit surface (see Ref. 6). One can then get the new values of the velocity c_τ and wall location c, by integrating $c_{\tau\tau}$.

V. Fixed Walls

In the case where the wall is fixed and prescribed, the computation of the pressure evolution is done on the basis of Eq. (2), where $\tilde{u}_\tau$ and $c_{\tau Z}$ are set equal to zero and p_τ is unknown. The velocity evolution is computed according to Eq. (5) and the new u,w components are obtained by the decoding done on the base of the prescribed slope of the wall. Finally, the energy equation provides the evolution of the entropy.

VI. Numerical Examples

Four examples of the method proposed herein are described. The first three refer to arbitrarily chosen pressure distributions. Once the inverse problem is solved, a check is performed with the direct (time-dependent) computation which takes as an input datum the wall geometry obtained from the previous inverse computation. The last example refers to the inverse computation of the analytically known Ringleb flow.[8] It provides a measure of the reliability of the method.

A. Two-Dimensional Subsonic Diffuser

The upper wall geometry of a two-dimensional diffuser has to be computed in order to satisfy the following pressure distribution along it:

$$p=0.85+0.05[1-\cos(z\pi/1.5)]$$

while its entry width and lower wall geometry are given.

Figure 3 shows the computed wall shape and inner flowfield. The solid lines refer to the isobars that result from the inverse computation. On the base of the wall geometry obtained in this way, the direct computation has been performed and the new isobars are denoted by the symbols (triangles).

Figure 4 shows the shape taken by the movable wall during the transient at different time steps K. At the starting condition ($K=0$) the movable wall is a straight line and the flowfield is considered as steady and uniform. The uniform pressure level is $p=0.85$. During the time interval $0<t<1$ ($0<K<30$) the pressure acting on the wall is gradually increased up to the prescribed value; because of that the inner flowfield is perturbed and the wall starts to move. At the beginning the wall moves down because of the pressure increase; a compression wave propagates inside the flowfield, reaches the opposite wall, and is then reflected back to the movable wall pushing it up. At the time step $K=600$ the flowfield reaches a new steady configuration and the wall assumes the final shape which satisfies the prescribed pressure distribution.

B. Two-Dimensional Transonic Nozzle

This example is similar to the previous one; the upper wall is movable while the lower one is fixed. Now the pressure distribution is given by:

$$p=0.85-0.275[1-\cos(z\pi/1.5)]$$

in order to have a transonic flowfield. The starting condition has been assumed different from the previous one: the pressure distribution is the prescribed one from the beginning ($K=0$), while the wall shape and the inner flowfield are guessed on the basis of the one-dimensional analysis.

Figure 5 shows the final shape of the nozzle and the isobar pattern. Here the triangles refer to the "check" direct computation.

C. The Intermediate Problem

This example refers to the case where one part of a wall has fixed geometry, while on the other the pressure is prescribed. A transonic axisymmetric nozzle is taken into consideration (see Fig. 6): it has a fixed conical wall ($0<z<0.5$) while on the remaining wall ($0.5<z<1.5$) the pressure is prescribed to be:

$$p=0.80-0.30\{1-\cos[(z-0.5)\pi]\}$$

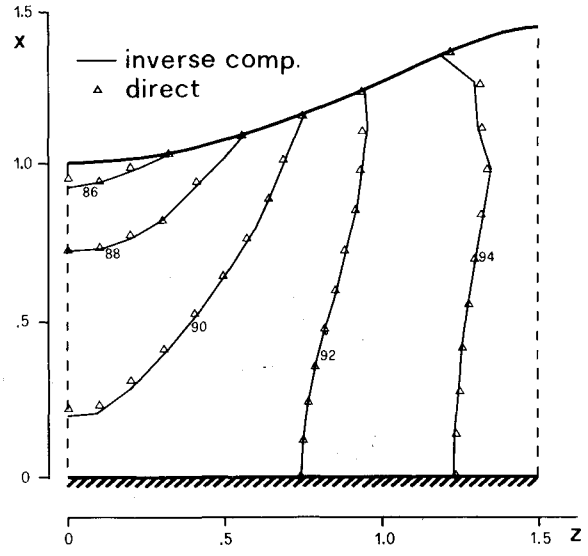

Fig. 3 Two-dimensional diffuser ($p^0 = 100$).

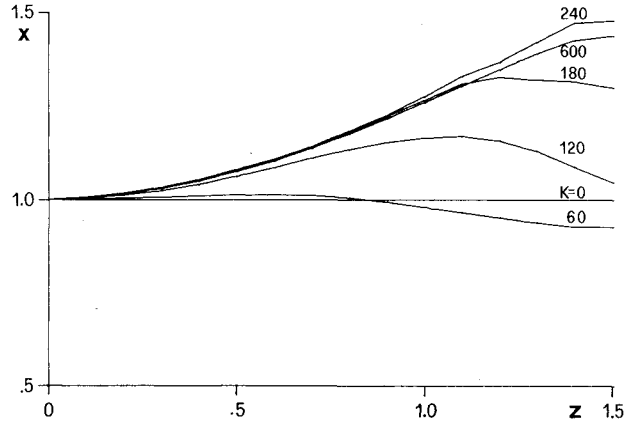

Fig. 4 Evolution in time of the moving wall (two-dimensional diffuser).

The starting condition has been assumed by the one-dimensional analysis, as in the previous example. The results of the inverse computation and the comparison with the corresponding direct computation are shown in Fig. 6.

Here, as well as in the previous examples, the mesh point distribution is 16×11.

D. Flow in an Elbow

The comparison between the numerical direct and inverse computation in the three previous examples is not completely meaningful. In fact, a comparison between two numerical procedures, based on the same numerical time-dependent technique, may be questionable. The present example has been performed in order to have a comparison with an analytically known flowfield. The Ringleb flow[8] is taken as the benchmark case. A set of streamlines ψ of the Ringleb flow are plotted in Fig. 7. Once two streamlines are selected, they may be regarded as the solid walls of an elbow, and, from the viewpoint of the inverse problem, the theoretical pressure acting on these may be taken as an input datum for an inverse problem.

As shown in Fig. 7, a polar frame of reference is used. The chosen channel is in the transonic region, and is confined by the streamlines $\psi = 0.8$, $\psi = 1.0$ and by the radial coordinate lines $\theta = 40$ deg, $\theta = 90$ deg.

The computational technique used in this case is obviously the same as that described in Sec. IV, with the trivial extension to the case of the polar coordinates.

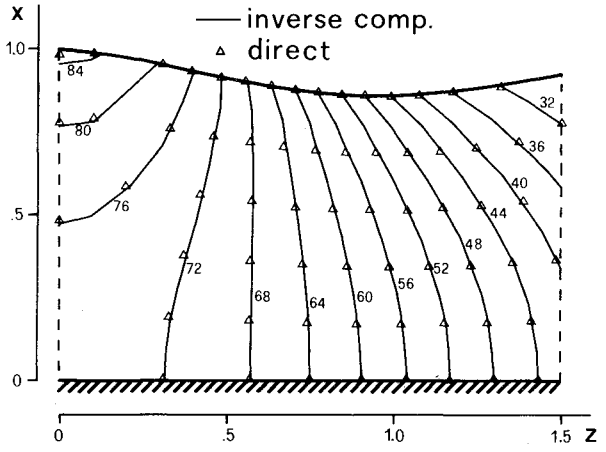

Fig. 5 Two-dimensional transonic nozzle ($p^0 = 100$).

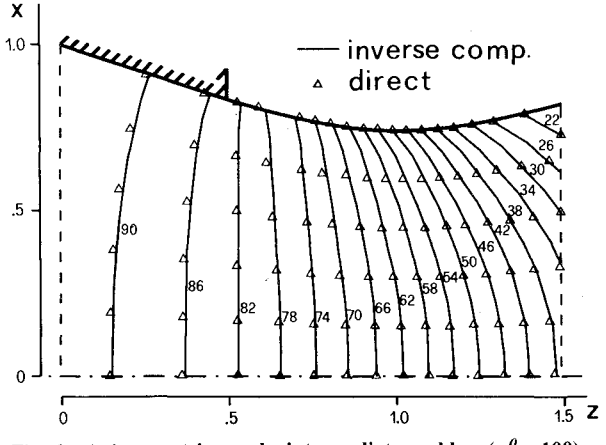

Fig. 6 Axisymmetric nozzle, intermediate problem ($p^0 = 100$).

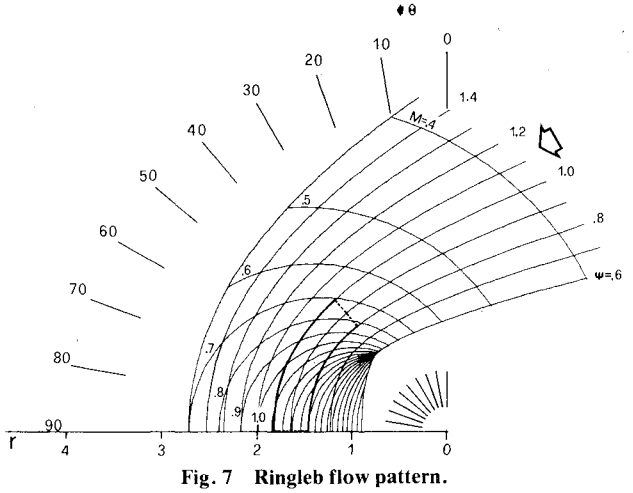

Fig. 7 Ringleb flow pattern.

Figure 8 shows the shapes of the walls during the transient. Both of them are assumed to be movable. Their shapes at the beginning of the computation ($K = 0$) are taken far from the theoretical ones, while the pressure acting on them is assumed the same as the theoretical one and is prescribed as function of the angle θ in the polar frame of reference. At the time step $K = 500$ the walls finally reach the steady locations. These are compared with the theoretical locations of the Ringleb flow streamlines, denoted by the symbols. No appreciable discrepancies appear. A more significant representation of this comparison is reported in Fig. 9, where the error of the locations of the walls is referred to as the channel width and is

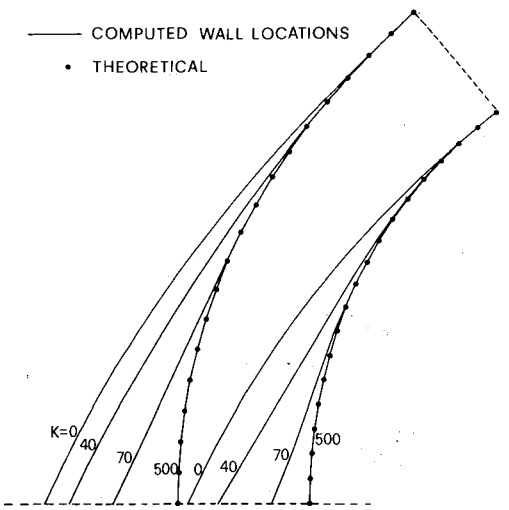

Fig. 8 Evolution in time of the moving walls (Ringleb flow).

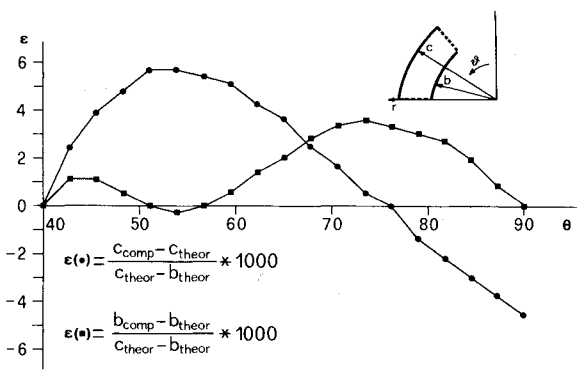

Fig. 9 Errors of the walls locations (Ringleb flow).

plotted along the channel. The largest discrepancy amounts is less than 0.6%.

To show how reliable this computation is, it is interesting to look at the properties of the flow in the channel as they are computed in the inverse computation. They may be compared with the theoretical ones (see Ref. 9). These errors, as regards the Mach number, are plotted in Fig. 10. Here the largest discrepancy amounts to an error of 0.4%. The mesh point distribution in this example is 19×7.

VII. Conclusions

A methodology for solving inverse problems in the case of internal flows has been presented. It allows for the treatment of inviscid subsonic and transonic flows.

The examples presented in this paper refer to two-dimensional and axisymmetric flows. The solutions are checked against the corresponding numerical solutions of the direct problem and against an analytically known flowfield. No conceptual and practical limitations exist to the extension to more general three-dimensional flows.

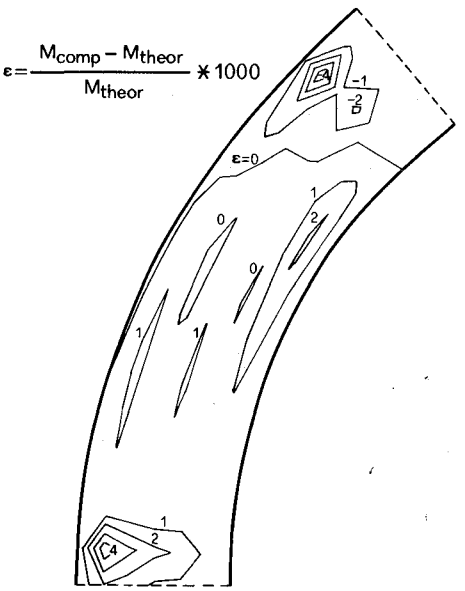

Fig. 10 Errors of the Mach number over the flowfield (Ringleb flow).

References

[1] Stanitz, J. D., "Design of Two-Dimensional Channels with Prescribed Velocity Distributions Along the Channel Walls," NACA Rept. 1115, 1953.

[2] Nelson, C. D., Hudson, W. G., and Yang, T., "The Design Performance of Axially Symmetrical Contoured Wall Diffusers Employing Suction Boundary Layer Control," ASME Paper 74-GT-152, 1974.

[3] Zannetti, L., "Transonic Flow Field in Two-Dimensional or Axisymmetric Convergent Nozzles," *Proceedings, 2nd GAMM Conference on Numerical Methods in Fluid Mechanics*, DFVLR, Oct. 1977, pp. 255-262.

[4] Moretti, G. and Abbett, M., "A Time-Dependent Computational Method for Blunt Body Flows," *AIAA Journal*, Vol. 4, Dec. 1966, pp. 2136-2138.

[5] McCormack, R. W., "The Effects of Viscosity in Hypervelocity Impact Cratering," AIAA Paper 69-354, 1969.

[6] Pandolfi, M. and Zannetti, L., "Some Permeable Boundaries in Mutidimensional Flows," 6th International Conference on Numerical Methods in Fluid Dynamics, Tbilisi, June 1978.

[7] Moretti, G., Pandolfi, M., "Entropy Layers," *Computers and Fluids*, Vol. 1, 1973, pp. 19-35.

[8] Ringleb, F., "Exacte Lösungen der Differential-gleichungen einer adiabatischen Gasströmung," *ZAMM*, Vol. 20, N. 4, 1940, pp. 785-798.

[9] Pandolfi, M. and Zannetti, L., 'Some Test on Finite Difference Algorithms for Computing Boundaries in Hyperbolic Flows," *GAMM Workshop,* University of Stüttgart, Feb. 1977; also, *Notes on Numerical Fluid Mechanics*, Vol. 1, pp. 68-88.